

## 10. DATA REPORT: IRON ISOTOPE GEOCHEMISTRY OF MID-CRETACEOUS ORGANIC-RICH SEDIMENTS AT DEMERARA RISE (ODP LEG 207)<sup>1</sup>

Robin E. Clayton,<sup>2, 3</sup> Alexandra J. Nederbragt,<sup>2</sup> Dmitry Malinovsky,<sup>4</sup> Per Andersson,<sup>5</sup> and Jürgen Thurow<sup>2</sup>

### ABSTRACT

Fe isotope measurements are presented for 10 samples from the Cenomanian–Turonian black shale unit in Hole 1260B at Demerara Rise. The samples bracket the latest Cenomanian ocean anoxic event and were selected to ascertain whether Fe isotopes can be used to gain a better understanding of oceanic redox conditions during the mid-Cretaceous. Three extraction procedures were used to provide Fe extracts that represent the Fe oxide (average  $Fe_{\text{CBD}} = 0.07$  wt%,  $N = 8$ ), Fe oxide-sulfide-carbonate (average  $Fe_{\text{AR}} = 0.34$  wt%,  $N = 10$ ), and total Fe fractions (average  $Fe_{\text{HF}} = 0.81$  wt%,  $N = 10$ ). Fe isotope measurements were conducted on all  $Fe_{\text{AR}}$  extracts as a priority as these were considered to best reflect changes in the redox environment.  $\delta^{56}\text{Fe}$  values range between  $0.02\text{‰} \pm 0.09\text{‰}$  and  $-0.77\text{‰} \pm 0.05\text{‰}$  and appear to correlate negatively with the C/N ratio and oxygen index of total organic carbon. Isotopic measurements of two Fe oxide ( $Fe_{\text{CBD}}$ ) extracts show a much heavier isotopic composition ( $\delta^{56}\text{Fe} = 0.74\text{‰} \pm 0.08\text{‰}$  and  $0.63\text{‰} \pm 0.04\text{‰}$ ), which suggests isotopic partitioning between different mineral components in the sediment.

<sup>1</sup>Clayton, R.E., Nederbragt, A.J., Malinovsky, D., Andersson, P., and Thurow, J., 2007. Data report: iron isotope geochemistry of mid-Cretaceous organic-rich sediments at Demerara Rise (ODP Leg 207). *In* Mosher, D.C., Erbacher, J., and Malone, M.J. (Eds.), *Proc. ODP, Sci. Results, 207*: College Station, TX (Ocean Drilling Program), 1–14. doi:10.2973/odp.proc.sr.207.109.2006

<sup>2</sup>Department of Earth Sciences, University College London, Gower Street, London WC1E 6BT, UK.

Correspondence author:  
[a.nederbragt@ucl.ac.uk](mailto:a.nederbragt@ucl.ac.uk)

<sup>3</sup>Deceased.

<sup>4</sup>Division of Applied Geology, Luleå University of Science and Technology, S-97187 Luleå, Sweden.

<sup>5</sup>Laboratory for Isotope Geology, Swedish Museum of Natural History, Box 50007, 10405 Stockholm, Sweden.

## INTRODUCTION

Stable isotope geochemistry of light elements (C, N, S, O, and H) is a recognized tool to reconstruct large-scale changes in global biogeochemical cycles from the Archaean onward. Over the past 5 yr, the stable isotopes of the transition elements have emerged as a novel and exciting development in the field of isotope geochemistry made possible by recent advances in multicollector inductively coupled plasma-mass spectrometers (ICP-MS). This is a rapidly expanding field of research that is only just beginning to address the physical, chemical, and biological driving forces for isotopic fractionation in nature. Iron is perhaps the most important transition element in (bio)geochemical processes and cycles. It is heavily implicated in contemporary paleoceanographic and paleoclimatological issues, such as the Fe fertilization hypothesis for the control of atmospheric carbon dioxide concentrations (Charette and Buesseler, 2000; Watson et al., 2000; Bakker et al., 2005).

There are four stable isotopes of Fe:  $^{54}\text{Fe}$  (5.84%),  $^{56}\text{Fe}$  (91.76%),  $^{57}\text{Fe}$  (2.12%), and  $^{58}\text{Fe}$  (0.28%), which show a mass-dependent fractionation of  $\sim 2\text{‰}$  per atomic mass unit. Iron is a redox-sensitive element (Fe reduction is a common terminal electron accepting process), and so the changes in redox conditions that affect Fe speciation are of fundamental importance. However, there is only rudimentary knowledge about the mechanisms of kinetic isotopic fractionation in response to these changes. In addition, only sparse information exists on the equilibrium fractionation of Fe isotopes during crystallization of simple inorganic phases. As new experimental data become available, more Fe isotope measurements on samples from the natural environment are required to assess how closely natural systems can be modeled in terms of environmental changes, such as changes in Eh-pH and oceanic anoxia. In particular, natural environments for which a coherent set of proxy information already exists are the most suitable to examine the fractionation of Fe isotopes in nature.

This preliminary study is concerned with the Fe isotope geochemistry in mid-Cretaceous organic-rich sediments at Demerara Rise and aims to explore whether Fe isotope geochemistry has potential to contribute to a better understanding of local and/or global redox processes during the mid-Cretaceous. Several ocean anoxic events (OAEs) occurred during the Jurassic and Cretaceous that represent periods with widespread anoxic conditions in the world's oceans and which had an impact on the oceanic Fe cycle. The Cenomanian–Turonian sequence on Demerara Rise recovered during Leg 207 was selected because it represents a combination of regional and global anoxia (Erbacher, Mosher, Malone, et al., 2004). Black shale deposition occurred throughout the Cenomanian and Turonian in a belt along the southern North Atlantic margin, while the world's oceans remained mainly oxic for most of this time interval. Global anoxia is represented by the latest Cenomanian OAE 2, when anoxic conditions were prevalent in much of the world's oceans. In theory, this makes the Demerara Rise sequence ideal to test if global vs. local effects on Fe isotope fractionation can be distinguished.

Our results are presented as a data report because only part of the planned measurements could be realized due to technical problems. These measurements, however, indicate that substantial fractionation of Fe isotopes did occur within the black shales, which in part can be correlated with a change in organic matter preservation. We investi-

gated the possibility that these isotopic variations are influenced by changes in oceanic redox conditions.

### Geochemistry of Fe Isotopes

Comparatively little is known about the possible fractionation mechanisms affecting Fe isotopes relative to our knowledge for isotopes of the lighter elements. With the exception of vital effects, temperature is the one principal control determining the magnitude of isotopic fractionation for C, N, O, and S. At atomic masses greater than ~50, the relative importance of temperature is diminished. Instead, other parameters known to play a subsidiary role for the lighter elements are implicated to have greater relative influence (Zhu et al., 2000). These include coordination chemistry, speciation, bond type, and redox conditions and can be generally categorized under “the bonding environment.” Recent studies continue to reaffirm large, low-temperature Fe isotope variation. Implicit in these data is the importance of redox- and biologically induced fractionation in controlling the relative Fe isotopic abundance in natural reservoirs.

In many circumstances Fe(III) species are isotopically heavier than reduced Fe(II) species, although the reverse occurs during some reactions (Matthews et al., 2001). Under experimental conditions that simulate reaction pathways thought to play a role in natural environments, enrichments in  $\delta^{56}\text{Fe}$  of 1.2‰–2.8‰ were found in Fe(III) relative to Fe(II) during inorganic and biological reactions (Beard et al., 1999; Anbar et al., 2000; Johnson et al., 2002; Croal et al., 2004; Icopini et al., 2004). Experiments have shown that for strictly inorganic systems, the bonding environment exerts a key influence in partitioning isotopes. But the relative dominance of kinetic or equilibrium processes remains poorly understood. Whereas it is relatively easy to generate a kinetic isotope fractionation during rapid precipitation of oxide minerals, experiments that demonstrate isotopic equilibrium are much harder to accomplish. So far, “equilibrium” fluid-mineral fractionations for Fe have been determined for

Fe(II) <sub>aq</sub> -hematite	=	-3.0‰ ± 0.3‰	(Skulan et al., 2002; Johnson et al., 2002; Welch et al., 2003).
Fe(III) <sub>aq</sub> -hematite	=	-0.1‰ ± 0.2‰	(Skulan et al., 2002).
Fe(II) <sub>aq</sub> -siderite	=	0.5‰ ± 0.2‰	(Wiesli et al., 2003).
Fe(II) <sub>aq</sub> -Fe(III) oxide	=	-0.9‰ ± 0.2‰	(Bullen et al., 2001).
Fe(III) <sub>aq</sub> -Fe(II) <sub>aq</sub>	=	2.9‰ ± 0.2‰	(Johnson et al., 2002; Welch et al., 2003).
Fe(II) <sub>aq</sub> -FeS	=	0.3‰ ± 0.05‰	(Butler et al., 2003).

Theoretical predictions of isotopic fractionation based on  $^{57}\text{Fe}$  Mossbauer spectroscopic data (Polyakov and Mineev, 2000) have forecast 3‰–4‰ equilibrium isotopic fractionation (siderite-pyrite and siderite-magnetite). From the information above it is evident that relatively large Fe isotope fractionations take place during reactions that involve a change in redox state.

In general, only the reduced Fe species (Fe[II]) is soluble in the present-day oxic conditions of most surface environments, unless low pH conditions prevail. Despite this, the solubility of Fe(II) is very low in near-neutral pH environments, such that Fe concentrations <1 nM prevail in much of the modern open ocean (Martin and Gordon, 1988; Johnson et al., 1997) and exert one of the principal influences that

limit marine productivity (Martin and Fitzwater, 1988). The residence time of Fe in the modern ocean is <200 yr, which is much shorter than the turnover rate of the global ocean (Broecker and Peng, 1982; Johnson et al., 1997). This implies that any fractionation of oceanic Fe will be dominated by local processes, as it does not remain long enough in solution for large-scale circulation processes to maintain isotopic contrasts between different water masses. Indeed, the Fe isotope composition of most modern Fe minerals is more or less constant at 0‰ and is indistinguishable from that of Fe in igneous rocks (Beard et al., 2003), indicating that isotope fractionation under modern (oxic) conditions plays a minor role. Loess, turbidites, fluvial particulates and organic carbon ( $C_{org}$ )-poor gray shales deposited under oxic conditions show a normal distribution of isotopic compositions with an average  $\delta^{56}\text{Fe}$  of ~0‰, similar to terrestrial igneous rocks. The largest fractionation found in the modern ocean occurs in hot hydrothermal vents along mid-ocean ridges and in ferromanganese crusts ( $\delta^{56}\text{Fe}$  about -0.4‰ and about -0.6‰, respectively) (Beard et al., 2003; Levasseur et al., 2004).

In contrast,  $C_{org}$ -rich black shales deposited and diagenetically modified under anoxic conditions show a wide range in isotopic composition and include some of the most negative  $\delta^{56}\text{Fe}$  values (Beard et al., 2003; Yamaguchi et al., 2003; Matthews et al., 2004). Fluctuations of  $\delta^{56}\text{Fe}$  ~4‰ are measured in late Archaean rocks (-2.5‰–1.0‰ [Johnson et al., 2003] or -3.5‰ to +0.5‰ [Rouxel et al., 2005]), in which  $\delta^{56}\text{Fe}$  values increase in the order pyrite-Fe carbonate-hematite-magnetite (Johnson et al., 2003). The large range of variability is attributed to a much larger pool of dissolved Fe(II), the result of the reducing conditions that existed in the late Archaean, whose isotope composition was fractionated globally by deposition of Fe oxides (Rouxel et al., 2005). The profound determining influence that redox has on the nature and abundance of Fe species and the large Fe isotopic fractionations that occur in response to changes in redox suggest that Fe isotopes may become a valuable proxy in paleoceanographic reconstructions.

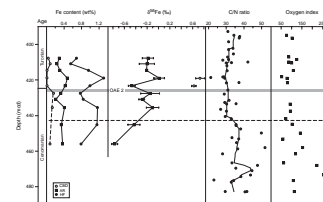
## MATERIAL AND METHODS

### Sample Material and Iron Extraction

Samples were collected from the Cenomanian–Turonian black shale unit in Hole 1260B based on shipboard stratigraphic data (Erbacher, Mosher, Malone, et al., 2004). Ten samples were selected for Fe isotope analysis between ~404 and 456 meters composite depth (mcd), bracketing the late Cenomanian OAE 2. Age assignment of the samples (Fig. F1) is based on stable carbon isotope stratigraphy established subsequently (Erbacher et al., 2005), which showed that the  $\delta^{13}\text{C}$  excursion defining OAE 2 is located between 424 and 426.5 mcd.

Bulk sediment samples were dried overnight at 50°C and powdered using an agate pestle and mortar. In these sediments, Fe is present within a number of mineralogical components, principally sulfide, carbonate, silicate, and oxide minerals. Three aliquots from the powdered samples were separated, and separate extractions were performed on each in order to extract Fe from the oxide-sulfide-carbonate and the oxide-only fractions, as well as a total digestion to extract Fe from all components except organic carbon (Tables T1, T2). The oxide fraction was

F1.  $\delta^{56}\text{Fe}$  values and abundance of iron vs. composite depth, p. 12.



T1. Sample preparation methods used for Fe extraction, p. 13.

T2. Iron extracted by different sample preparation methods, p. 14.

selectively extracted using the Na citrate-Na bicarbonate-dithionite (CBD) ( $\text{Fe}_{\text{CBD}}$ ) method (Hunt et al., 1995; van Oorschot and Dekkers, 1999), the oxide-sulfide-carbonate fraction was extracted using an aqua regia (AR) leach ( $\text{Fe}_{\text{AR}}$ ), and the total digestion was performed using  $\text{HNO}_3$ -HF ( $\text{Fe}_{\text{HF}}$ ). All sediment residues were dried after extraction and weighed to determine the mass of sample dissolved.

The CBD method (Mehra and Jackson, 1960) is based on reductive Fe oxide dissolution with dithionite ( $\text{Na}_2\text{S}_2\text{O}_4$ ) as the reductant and Na citrate ( $\text{Na}_3\text{C}_6\text{H}_5\text{O}_7 \cdot 2\text{H}_2\text{O}$ ) as a chelating agent to bind the dissolved Fe. Sodium bicarbonate ( $\text{NaHCO}_3$ ) is used to buffer the  $\text{H}^+$  loss during the reaction. The reductive solution of Fe oxides is a kinetic process and factors such as pH, crystallinity, and temperature have a major effect on the dissolution rate.

### Anion Exchange Chemistry

Samples dissolved in 7-M HCl were purified by anion exchange using analytical grade macroporous resin (AG MP-1), based on a procedure described by Maréchal et al. (1999) in which quantitative yields for Fe were reported. The majority of matrix elements were washed off the column with 24 mL of 7-M HCl, after which the Fe was eluted in 10 mL of 2-M HCl. The purified Fe solutions were evaporated to dryness, redissolved in 200  $\mu\text{L}$  of concentrated  $\text{HNO}_3$ , and made up to a volume of 10 mL with deionized water prior to screening for isobaric interferences on the masses of interest, particularly  $^{54}\text{Cr}$ , using a single-collector magnetic sector ICP-MS (Thermo Finnigan Element 2) operated in low- and medium-resolution modes. The raw data were blank corrected and normalized using indium (In) as the internal standard, from which Fe concentrations were calculated offline. Procedural blanks were always  $<36$  ng Fe.

### Mass Spectrometry

Iron isotope ratio measurements were performed using MC ICP-MS (Neptune, Thermo Finnigan) provided by High Lat resources (HPRI-CT-2001-00125) through the European Commissions "Access to Research Infrastructure" action of the Improving Potential Programme. The operating conditions adopted for the instrument follow the protocols described in Malinovsky et al. (2003) and Andrén et al. (2004). Detailed description of the procedure for optimization of ion lens settings and sampling depth in order to obtain lower instrumental uncertainty and higher mass bias stability is given in Andrén et al. (2004). The Neptune was operated in high-resolution mode ( $R = \sim 9000$ ) throughout this study to resolve the Fe isotopes from the major spectral interferences:

- $^{54}\text{Fe}$ :  $^{54}\text{Cr}$  and  $^{40}\text{Ar}^{14}\text{N}^+$ .
- $^{56}\text{Fe}$ :  $^{40}\text{Ar}^{16}\text{O}^+$ ,  $^{40}\text{Ca}^{16}\text{O}^+$ , and  $^{40}\text{K}^{16}\text{O}^+$ .
- $^{57}\text{Fe}$ :  $^{40}\text{Ar}^{16}\text{OH}^+$  and  $^{40}\text{Ca}^{16}\text{OH}^+$ .
- $^{58}\text{Fe}$ :  $^{58}\text{Ni}$ .

The isotopes that were collected are  $^{54}(\text{Fe} + \text{Cr})$ ,  $^{56}\text{Fe}$ ,  $^{57}\text{Fe}$ ,  $^{58}(\text{Fe} + \text{Ni})$ ,  $^{60}\text{Ni}$ , and  $^{62}\text{Ni}$ . All analyses were made in an alternating sequence of samples and isotope standards (IRMM-014 Fe isotope standard). Maximum error in the  $^{56}\text{Fe}/^{54}\text{Fe}$  ratio caused by  $^{54}\text{Cr}$  remaining after the anion exchange separation was assessed to be  $<0.005\%$ . No attempt was made to deter-

mine the  $^{58}\text{Fe}$  isotope because Ni was used as an internal standard for mass discrimination correction.

Samples and isotope standards were prepared at 5 ppm and spiked with 5 ppm Ni in 0.3-M  $\text{HNO}_3$ . Ni doping allows a correction algorithm to be applied for mass discrimination effects in the plasma source using the mass discrimination factor ( $f_{\text{Ni}}$ ) determined from the  $^{62}\text{Ni}/^{60}\text{Ni}$  measurement. Linearity between the mass discrimination factors,  $f_{\text{Ni}}$  and  $f_{\text{Fe}}$ , is assumed constant during one measurement session according to the exponential correction employed (Woodhead, 2002), although between sessions the variation between mass discrimination factors can be significant. Data were corrected for mass discrimination effects using a procedure based on that described in Maréchal et al. (1999), Albarède et al. (2004), and Albarède and Beard (2004). By combining standard-sample bracketing with Ni doping (Anbar et al., 2001; Cardinal et al., 2003), mass discrimination factors are calculated for each standard-sample data set acquired over a short measurement interval, substantially reducing the effect on the data from variation in mass bias that occurs over time.

Isotopic data were processed using a combination of online baseline subtraction, calculation of ion beam intensity ratios, and outlier filtering by a  $2\sigma$  test. Further statistical treatment and mass bias corrections were performed offline. The internal analytical precision on the measured ratios was  $>50$  ppm for the  $^{56}\text{Fe}/^{54}\text{Fe}$  ratio and  $>100$  ppm for the  $^{57}\text{Fe}/^{54}\text{Fe}$  ratio at 1 standard deviation ( $\sigma$ ) level. The external precision on repeated measurements of the IRMM-014 Fe isotope standard using the raw  $^{56}\text{Fe}/^{54}\text{Fe}$  ratios was typically  $\sim 450$  ppm ( $2\sigma$ ). Isotopic variation in  $^{56}\text{Fe}/^{54}\text{Fe}$  is expressed as permil variation relative to IRMM-014 ( $^{56}\text{Fe}/^{54}\text{Fe} = 15.69859 \pm 0.00027$ ) using the standard  $\delta$  notation ( $\delta^{56}\text{Fe}$ ).

## RESULTS

Iron concentrations and isotope values are reported in Table T2. Results are plotted against stratigraphic depth in Figure F1 and compared to selected shipboard organic geochemical data.

### Iron Concentrations

The amount of elemental Fe obtained by  $\text{HNO}_3$ -HF ( $\text{Fe}_{\text{HF}}$ ) digestion ranges between 0.6 and 1.3 wt%. The average sample mass digested during this procedure was 82% (range = 73%–87%), indicating that much of the lithogenic material was consumed and that  $\text{Fe}_{\text{HF}}$  essentially represents the total amount of Fe within the sediment. The residue from these extractions should consist mostly of organic matter. The total organic carbon content in the Cenomanian–Turonian organic-rich levels that were sampled in Hole 1260B varies  $\sim 10$  wt% (Erbacher, Mosher, Malone, et al., 2004), which corresponds to a proportionally higher percentage of organic matter when other elements (H, O, and S) are taken into account. The AR digestion extracted between 0.2 and 0.5 wt% Fe (mean = 0.34%) or between 25% and 46% of the total Fe in the sample. Iron-sulfides, Fe oxides, and any Fe carbonates are dissolved during this procedure. Shipboard analyses of smear slides showed that pyrite, which is the main component expected in  $\text{Fe}_{\text{AR}}$  extracts, occurs in variable concentrations downhole to the base Core 207-1260A-44R but is rare or absent lower in the black shale unit. The low abundance of mi-

microscopically identifiable pyrite agrees with the relatively low  $Fe_{AR}$  values that were obtained. At this stage in our studies, we cannot evaluate the relative importance of Fe carbonate; however, the minor proportion of loosely bound Fe and that contained in the oxide fraction would have been consumed.

With the exception of two samples, the amount of Fe extracted by the CBD method yielded low to very low Fe concentrations (between 0.009% and 0.16%, mean = 0.07%,  $n = 8$ ), such that  $Fe_{CBD}$  concentrations range from 2% to 49% of  $Fe_{AR}$ . The two anomalously high  $Fe_{CBD}$  yields that were obtained are the result of failure in the anion exchange procedure, manifested by abnormal discoloration, and behavior of the AG MP-1 resin bed during Fe separation. A negligible difference in sample mass before and after CBD extraction is found; in some samples, a small increase in mass was measured, presumably because of precipitation of Na that is present in the CBD mixture. From the negligible mass difference, it is assumed that the CBD extraction did not dissolve any Fe carbonate. Calcite is a major component of the sediment, and any dissolution of carbonates would have resulted in more significant losses from sample mass. The low  $Fe_{CBD}$  concentrations indicate that Fe oxides are rare, as would be expected under the anoxic conditions that predominated during the mid-Cretaceous at Demerara Rise.

### Fe Isotope Compositions

The  $\delta^{56}Fe$  values for  $Fe_{AR}$  extracts range between 0.02‰ and -0.77‰ and, except for the three lightest extracts ( $\delta^{56}Fe = -0.47‰ \pm 0.06‰$ ,  $-0.43‰ \pm 0.11‰$ , and  $-0.77‰ \pm 0.05‰$ ), correspond to Fe concentration ( $r = 0.96$ ). This correlation may reflect increasing amounts of Fe leached from the silicate fraction of the sediment, which results in the isotopic composition corresponding more closely to the global average isotopic composition of Fe ( $\delta^{56}Fe = 0‰$ ). There is no correlation between  $\delta^{56}Fe$  and weight percent dissolved sample or between  $\delta^{56}Fe$  and weight percent  $Fe_{CBD}$ . The three lightest extracts may represent significant reduced Fe in another mineral component not represented in the other seven extracts or in a different proportion of Fe sulfide and Fe carbonate relative to each other. Unfortunately, the isotopic composition of only two  $Fe_{CBD}$  extracts was measured. Both  $Fe_{CBD}$  measurements are significantly heavier compared with the isotopic composition of the corresponding  $Fe_{AR}$  extracts, yielding positive  $\delta^{56}Fe$  values of 0.73‰ (Sample 207-1260A-46R-2, 31–32 cm) and  $0.63‰ \pm 0.04‰$  (Sample 46R-5, 53–54 cm). These values are ~0.7‰ heavier than the global average Fe isotope composition of  $\delta^{56}Fe = 0‰$  (Beard et al., 2003). Therefore, it is unlikely that the three lightest  $Fe_{AR}$  extracts are the result of a Fe oxide component but instead may represent a diagenetic component precipitated from reduced Fe(II)-bearing pore waters or biologically mediated Fe that is not present in the other AR extracts.

Comparison of the  $Fe_{AR}$  with  $Fe_{CBD}$  extractions for Samples 207-1260A-46R-2, 31–32 cm, and 46R-5, 53–54 cm, reveals a difference in  $\delta^{56}Fe$  of 0.72‰ and 1.10‰, respectively, between  $\delta^{56}Fe_{CBD}$  and  $\delta^{56}Fe_{AR}$ . These values qualitatively represent the difference between the Fe oxide and AR-extractable mineral components in the sediment. A mass balance correction for the presence of Fe oxides in the  $Fe_{AR}$  extract can be performed assuming that all CBD-extractable Fe is also extracted by AR:

$$a \times \delta^{56}Fe_{CBD} + (1 - a) \times \delta^{56}Fe_{AR-CBD} = \delta^{56}Fe_{AR}$$

in which  $a$  is the percentage of  $\text{Fe}_{\text{CBD}}$  relative to  $\text{Fe}_{\text{AR}}$ . Resulting values for  $\delta^{56}\text{Fe}_{\text{AR-CBD}}$  are  $-0.002\text{‰}$  in Sample 207-1260A-46R-2, 31–32 cm, and  $-0.49\text{‰}$  in Sample 46R-5, 53–54 cm. This results in a corrected  $\text{Fe}_{\text{AR-CBD}}$  that is only  $\sim 0.02\text{‰}$  lighter than the measured  $\text{Fe}_{\text{AR}}$  because of the low concentration of  $\text{Fe}_{\text{CBD}}$  in these two samples. This indicates an isotopic difference between the Fe oxide (Fe[III]) and Fe sulfide + Fe carbonate (Fe[II]) components in the sediment of between  $0.75\text{‰}$  and  $1.12\text{‰}$ .

The  $\delta^{56}\text{Fe}$  variation between different mineralogical components may reflect redox cycling in the sediments of Demerara Rise, which may include reduction by interaction with dissolved  $\text{H}_2\text{S}$  and bacterial processing. The reduction of Fe by bacteria produces isotopically light  $\text{Fe(II)}_{\text{aq}}$ , and the equilibrium fractionation between this and  $\text{Fe(III)}_{\text{aq}}$  in low-pH environments has been shown by experiment to be negative (Johnson et al., 2002, 2004; Welch et al., 2003). Severmann et al. (2002) measured  $\text{Fe(II)}_{\text{aq}}$  as low as  $\delta^{56}\text{Fe} = -5.0\text{‰}$  in pore fluids from  $\text{C}_{\text{org}}$ -rich sediments. Experimental studies have indicated that Fe isotope fractionation between  $\text{FeCO}_3\text{-Fe(II)}_{\text{aq}}$  and  $\text{FeS-Fe(II)}_{\text{aq}}$  partitions the lighter isotope into the solid phase (Wiesli et al., 2003; Butler et al., 2003), suggesting that diagenetically precipitated minerals will be isotopically light in reducing environments. It is likely that the Fe isotopic compositions measured in the Demerara Rise sediments reflect partitioning between different mineral components and  $\text{Fe(II)}_{\text{aq}}$  under changing redox conditions and that there is indeed a change in redox conditions within the section is indicated by shipboard C/N ratios and oxygen index (OI) values. Two of the three samples with light  $\delta^{56}\text{Fe}_{\text{AR}}$  values are located below 442 mcd, at which level there is a change in organic matter preservation. On average, high C/N ratios and OI values are found below 442 mcd, indicating that organic matter is more degraded and contains a higher portion of inert material than in the upper part of the section (Erbacher, Mosher, Malone, et al., 2004); hydrogen index values are high also, which indicates that the organic matter is of marine origin, not terrigenous. The shift in organic matter preservation points to a change in bacterial action, which may have affected the partitioning of Fe within the sediment.

## **ACKNOWLEDGMENTS**

This research used samples and data provided by the Ocean Drilling Program (ODP). ODP is sponsored by the U.S. National Science Foundation (NSF) and participating countries under management of Joint Oceanographic Institutions (JOI), Inc. Financial support by High Lat resources (HPRI-CT-2001-00125) through the European Commissions "Access to Research Infrastructure" action of the Improving Potential Programme is acknowledged. R.E. Clayton acknowledged research funding from The Royal Society, United Kingdom (grant number 21380).

## REFERENCES

- Albarède, F., and Beard, B.L., 2004. Analytical methods for non-traditional isotopes. In Johnson, C.M., Beard, B.L., and Albarède, F. (Eds.), *Geochemistry of Non-Traditional Stable Isotopes*. Rev. Mineral. Geochem., 55:113–152.
- Albarède, F., Télouk, P., Blichert-Toft, J., Boyet, M., Agranier, A., and Nelson, B., 2004. Precise and accurate isotopic measurements using multiple-collector ICPMS. *Geochim. Cosmochim. Acta*, 68(12):2725–2744. doi:10.1016/j.gca.2003.11.024
- Anbar, A.D., Knab, K.A., and Barling, J., 2001. Precise determination of mass-dependent variations in the isotopic composition of molybdenum using MC-ICPMS. *Anal. Chem.*, 73(7):1425–1431. doi:10.1021/ac000829w
- Anbar, A.D., Roe, J.E., Barling, J., and Neelson, K.H., 2000. Nonbiological fractionation of iron isotopes. *Science*, 288(5463):126–128. doi:10.1126/science.288.5463.126
- Andrén, H., Rodushkin, I., Stenberg, A., Malinovsky, D., and Baxter, D.C., 2004. Sources of mass bias and isotope ratio variation in multi-collector ICP-MS: optimization of instrumental parameters based on experimental observations. *J. Anal. At. Spectrom.*, 19(9):1217–1224. doi:10.1039/b403938f
- Bakker, D.C.E., Bozec, Y., Nightingale, P.D., Goldson, L., Messias, M.-J., de Baar, H.J.W., Liddicoat, M., Skjelvan, I., Strass, V., and Watson, A.J., 2005. Iron and mixing affect biological carbon uptake in SOIREE and EisenEx, two Southern Ocean iron fertilisation experiments. *Deep-Sea Res., Part I*, 52(6):1001–1019. doi:10.1016/j.dsr.2004.11.015
- Beard, B.L., Johnson, C.M., Cox, L., Sun, H., Neelson, K.H., and Aguilar, C., 1999. Iron isotope biosignatures. *Science*, 285(5435):1889–1892. doi:10.1126/science.285.5435.1889
- Beard, B.L., Johnson, C.M., Von Damm, K.L., and Poulson, R.L., 2003. Iron isotope constraints on Fe cycling and mass balance in oxygenated Earth oceans. *Geology*, 31(7):629–632. doi:10.1130/0091-7613(2003)031<0629:IICOFC>2.0.CO;2
- Broecker, W.S., and Peng, T.-H., 1982. *Tracers in the Sea*: Palisades, NY (Eldigio Press).
- Bullen, T.D., White, A.F., Childs, C.W., Vivet, D.V., and Schultz, M.S., 2001. Demonstration of significant abiotic iron isotope fractionation in nature. *Geology*, 29(8):699–702. doi:10.1130/0091-7613(2001)029<0699:DOSAII>2.0.CO;2
- Butler, I.P., Archer, C., Rickard, D., Vance, V., and Oldroyd, A., 2003. Fe isotope fractionation during Fe(II) monosulfide precipitation from aqueous Fe solutions at pH 8 and ambient temperature. *Geochim. Cosmochim. Acta*, 67(18)(Suppl.):A51. (Abstract) doi:10.1016/S0016-7037(03)00506-4
- Cardinal, D., Alleman, L.Y., de Jong, J., Ziegler, K., and André, L., 2003. Isotopic composition of silicon measured by multicollector plasma source mass spectrometry in dry plasma mode. *J. Anal. At. Spectrom.*, 18(3):213–218. doi:10.1039/b210109b
- Charette, M.A., and Buesseler, K.O., 2000. Does iron fertilization lead to rapid carbon export in the Southern Ocean? *Geochem., Geophys., Geosyst.*, 1(10). doi:10.1029/2000GC000069
- Croal, L.R., Johnson, C.M., Beard, B.L., and Newman, D.K., 2004. Iron isotope fractionation by Fe(II)-oxidizing photoautotrophic bacteria. *Geochim. Cosmochim. Acta*, 68(6):1227–1242. doi:10.1016/j.gca.2003.09.011
- Erbacher, J., Friedrich, O., Wilson, P.A., Birch, H., and Mutterlose, J., 2005. Stable organic carbon isotope stratigraphy across Oceanic Anoxic Event 2 of Demerara Rise, western tropical Atlantic. *Geochem., Geophys., Geosyst.*, 6(6):Q06010. doi:10.1029/2004GC000850
- Erbacher, J., Mosher, D.C., Malone, M.J., et al., 2004. *Proc. ODP, Init. Repts.*, 207: College Station, TX (Ocean Drilling Program). doi:10.2973/odp.proc.ir.207.2004
- Hunt, C.P., Singer, M.J., Kletetschka, G., TenPas, J., and Verosub, K.L., 1995. Effect of citrate-bicarbonate-dithionite treatment on fine-grained magnetite and

- maghemite. *Earth Planet. Sci. Lett.*, 130(1–4):87–94. doi:10.1016/0012-821X(94)00256-X
- Icopini, G.A., Anbar, A.D., Ruebush, S.S., Tien, M., and Brantley, S.L., 2004. Iron isotope fractionation during microbial reduction of iron: the importance of adsorption. *Geology*, 32(3):205–208. doi:10.1130/G20184.1
- Johnson, C.M., Beard, B.L., and Albarede, F., (Eds.), 2004. *Geochemistry of Non-Traditional Stable Isotopes*. Rev. Mineral. Geochem., 55.
- Johnson, C.M., Beard, B.L., Beukes, N.J., Klein, C., and O’Leary, J.M., 2003. Ancient geochemical cycling in the Earth as inferred from Fe isotope studies of banded iron formations from the Transvaal Craton. *Contrib. Mineral. Petrol.*, 144:523–547.
- Johnson, C.M., Skulan, J.L., Beard, B.L., Sun, H., Neilson, K.H., and Braterman, P.S., 2002. Isotopic fractionation between Fe(III) and Fe(II) in aqueous solutions. *Earth Planet. Sci. Lett.*, 195(1–2):141–153. doi:10.1016/S0012-821X(01)00581-7
- Johnson, K.S., Gordon, R.M., and Coale, K.H., 1997. What controls dissolved iron concentrations in the world ocean? *Mar. Chem.*, 57(3–4):137–161. doi:10.1016/S0304-4203(97)00043-1
- Levasseur, S., Frank, M., Hein, J.R., and Halliday, A.N., 2004. The global variation in the iron isotope composition of marine hydrogenetic ferromanganese deposits: implications for seawater chemistry? *Earth Planet. Sci. Lett.*, 224(1–2):91–105. doi:10.1016/j.epsl.2004.05.010
- Malinovsky, D., Stenberg, A., Rodushkin, I., Andren, H., Ingri, J., Öhlander, B., and Baxter, D.C., 2003. Performance of high resolution MC-ICP-MS for Fe isotope ratio measurements in sedimentary geological materials. *J. Anal. At. Spectrom.*, 18(7):687–695. doi:10.1039/b302312e
- Maréchal, C.N., Télouk, P., and Albarède, F., 1999. Precise analysis of copper and zinc isotope compositions by plasma-source mass spectrometry. *Chem. Geol.*, 156(1–4):251–273. doi:10.1016/S0009-2541(98)00191-0
- Martin, J.H., and Fitzwater, S.E., 1988. Iron deficiency limits phytoplankton growth in the north-east Pacific subarctic. *Nature (London, U. K.)*, 331(6154):341–343. doi:10.1038/331341a0
- Martin, J.H., and Gordon, R.M., 1988. Northeast Pacific iron distributions in relation to phytoplankton productivity. *Deep-Sea Res., Part A*, 35(2):177–196. doi:10.1016/0198-0149(88)90035-0
- Matthews, A., Morgans-Bell, H.S., Emmanuel, S., Jenkyns, H.C., Erel, Y., and Halicz, L., 2004. Controls on iron-isotope fractionation in organic-rich sediments (Kimmeridge Clay, Upper Jurassic, Southern England). *Geochim. Cosmochim. Acta*, 68(14):3107–3123. doi:10.1016/j.gca.2004.01.019
- Matthews, A., Zhu, X.-K., and O’Nions, K., 2001. Kinetic iron stable isotope fractionation between iron (-II) and (-III) complexes in solution. *Earth Planet. Sci. Lett.*, 192(1):81–92. doi:10.1016/S0012-821X(01)00432-0
- Mehra, O.P., and Jackson, M.L., 1960. Iron oxide removal from soils and clays by a dithionite-citrate system buffered with sodium bicarbonate. *Clays Clay Miner.*, 7:317–327.
- Polyakov, V.B., and Mineev, S.D., 2000. The use of Mössbauer spectroscopy in stable isotope geochemistry. *Geochim. Cosmochim. Acta*, 64(5):849–865. doi:10.1016/S0016-7037(99)00329-4
- Rouxel, O.J., Bekker, A., and Edwards, K.J., 2005. Iron isotope constraints on the Archean and Paleoproterozoic ocean redox state. *Science*, 307(5712):1088–1091. doi:10.1126/science.1105692
- Severmann, S., Larsen, O., Palmer, M.R., and Nüster, J., 2002. The isotopic signature of Fe-mineralization during early diagenesis. *Geochim. Cosmochim. Acta*, 66:A698.
- Skulan, J.L., Beard, B.L., and Johnson, C.M., 2002. Kinetic and equilibrium Fe isotope fractionation between aqueous Fe(III) and hematite. *Geochim. Cosmochim. Acta*, 66(17):2995–3015. doi:10.1016/S0016-7037(02)00902-X
- van Oorschot, I.H.M., and Dekkers, M.J., 1999. Dissolution behaviour of fine-grained magnetite and maghemite in the citrate-bicarbonate-dithionite extraction

- method. *Earth Planet. Sci. Lett.*, 167(3–4):283–295. doi:10.1016/S0012-821X(99)00033-3
- Watson, A.J., Bakker, D.C.E., Ridgwell, A.J., Boyd, P.W., and Law, C.S., 2000. Effect of iron supply on Southern Ocean CO<sub>2</sub> uptake and implications for glacial atmospheric CO<sub>2</sub>. *Nature (London, U. K.)*, 407(6805):730–733. doi:10.1038/35037561
- Welch, S.A., Beard, B.L., Johnson, C.M., and Braterman, P.S., 2003. Kinetic and equilibrium Fe isotope fractionation between aqueous Fe(II) and Fe(III). *Geochim. Cosmochim. Acta*, 67(22):4231–4250. doi:10.1016/S0016-7037(03)00266-7
- Wiesli, R.A., Beard, B.L., and Johnson, C.M., 2003. Experimental determination of Fe isotope fractionation between aq. Fe(II), “green rust” and siderite. *Geochim. Cosmochim. Acta*, 67:A533.
- Woodhead, J., 2002. A simple method for obtaining highly accurate Pb isotope data by MC-ICP-MS. *J. Anal. At. Spectrom.*, 17(10):1381–1385. doi:10.1039/b205045e
- Yamaguchi, K.E., Beard, B.L., Johnson, C.M., Ohkouchi, N., and Ohmoto, H., 2003. Iron isotope evidence for redox stratification of the Archaean Oceans. *Geochim. Cosmochim. Acta*, 67(Suppl. 1):A550.
- Zhu, X-K., O’Nions, R.K., Guo, Y., and Reynolds, B.C., 2000. Secular variation of iron isotopes in North Atlantic deep water. *Science*, 287(5460):2000–2002. doi:10.1126/science.287.5460.2000

**Figure F1.** Plot of  $\delta^{56}\text{Fe}$  values and the abundance of iron vs. composite depth, compared to organic matter C/N ratios and oxygen index (OI) from Erbacher, Mosher, Malone, et al. (2004). See text for explanation of different iron extraction methods. Error bars on Fe isotope values =  $2\sigma$ . Gray bar through plot denotes the stratigraphic extent of oceanic anoxic event (OAE) 2 as recognized from the  $\delta^{13}\text{C}$  stratigraphy of Erbacher et al. (2005). Horizontal dotted line = level at which organic matter preservation changes as indicated by the shift in average C/N and OI values. CBD = Na citrate-Na bicarbonate-dithionite, AR = aqua regia, HF = hydrofluoric acid.

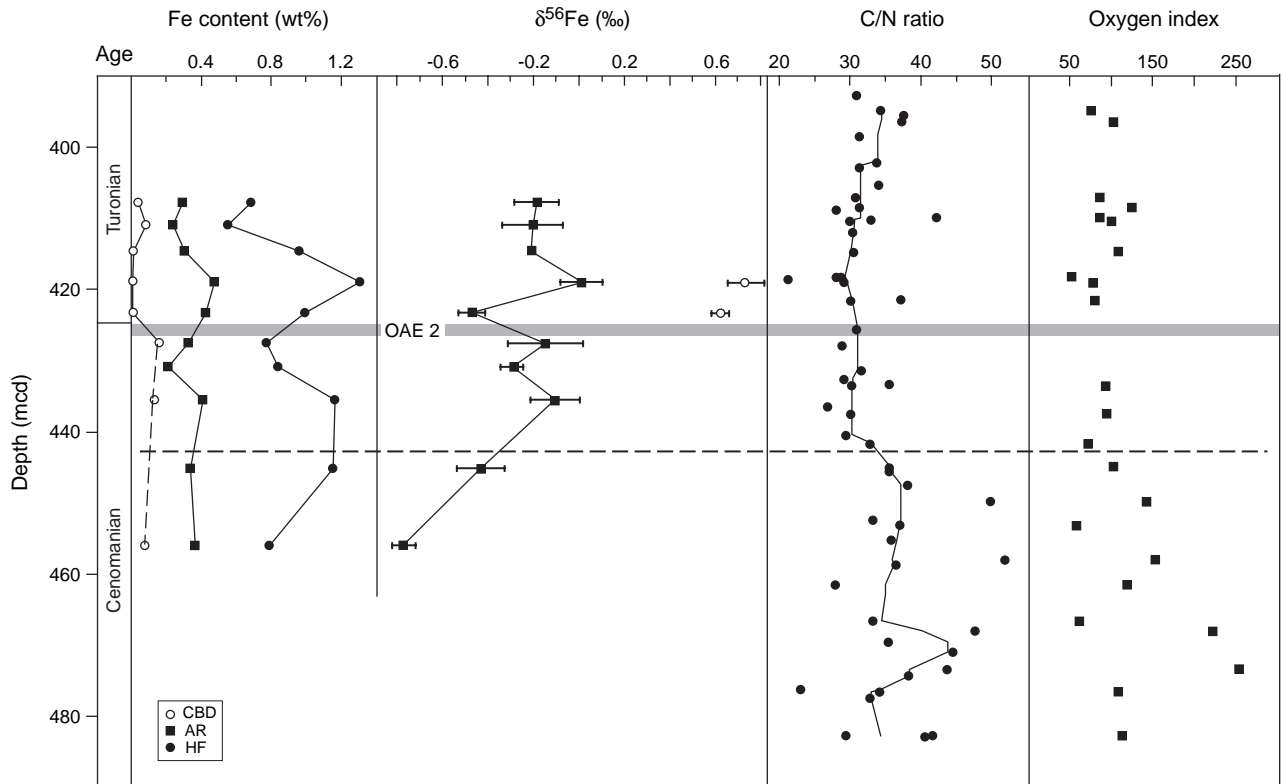


**Table T1.** Sample preparation methods used for the extraction of Fe from different sediment components.

Step	Fe oxide extraction ( $\text{Na}_3\text{C}_6\text{H}_5\text{O}_7 \cdot 2\text{H}_2\text{O} - \text{NaHCO}_3 - \text{Na}_2\text{S}_2\text{O}_4$ )	Sulfide-carbonate leach procedure (aqua regia)	Total digestion ( $\text{HNO}_3$ -HF)
1	Add 10 mL 0.3-M Na citrate solution + 1.25 mL 1-M Na bicarbonate solution	Add 1 mL 1-M HCl to consume carbonate	Add 2 mL conc. $\text{HNO}_3$ + 5 mL conc. HF
2	Heat solution overnight at 70°–75°C	Add 3 mL 7-M HCl	Heat on hot plate at 125°C for 36 hr in closed Teflon vessel
3	Add 0.5 g Na dithionite and stir for 15 s	Add 1 mL $\text{HNO}_3$	Evaporate to dryness at 75°C
4	Maintain at constant temperature for 15 min and stir every 5 min	Heat on hot plate at 125°C for 24 hr in closed Teflon vessel	Redissolve in 2 mL conc. $\text{HNO}_3$
5	Centrifuge 30 min at 4000 rpm	Evaporate to dryness at 75°C	Evaporate to dryness at 75°C
6	Decant and rinse residue with $\text{H}_2\text{O}$ , centrifuge 30 min at 4000 rpm	Redissolve in 2 mL 7-M HCl	Redissolve in 6 mL 7-M HCl
7	Evaporate under air in closed Teflon chamber (Aliquot 1)	Repeat Steps 5 and 6	Evaporate to dryness at 75°C
8	Repeat Steps 1–7 on residue (Aliquot 2)	Centrifuge 20 min at 4000 rpm	Redissolve in 2 mL 7-M HCl
9	Redissolve Aliquots 1 and 2 in 7-M HCl and combine		Centrifuge 20 min at 4000 rpm
10	Centrifuge 30 min at 4000 rpm		

**Table T2.** Amount of iron extracted by different sample preparation methods and the stable isotope composition.

Hole, core, section, interval (cm)	Depth (mcd)	CBD extraction*			AR extraction				HNO <sub>3</sub> -HF	
		Fe (wt%)	δ <sup>56</sup> Fe (‰)	2σ†	Fe (wt%)	Percent digested	δ <sup>56</sup> Fe (‰)	2σ	Fe (wt%)	Percent digested
207-										
1260A-44R-1, 93-94	407.75	0.05	—		0.30	29	-0.18	0.10	0.69	73
1260A-44R-4, 32.5-33.5	410.95	0.09	—		0.24	46	-0.20	0.14	0.56	78
1260A-45R-3, 27-28	414.59	0.02	—		0.31	21	-0.21	0.01	0.97	80
1260A-46R-2, 31-32	418.93	0.01	0.74	0.08	0.48	9	0.02	0.09	1.31	87
1260A-46R-5, 53-54	423.24	0.01	0.63	0.04	0.43	23	-0.47	0.06	0.10	86
1260B-35R-6, 21-22	427.50	0.16	—		0.33	40	-0.14	0.18	0.78	83
1260A-47R-3, 33-34	430.82	0.72‡	—		0.21	31	-0.29	0.05	0.84	84
1260A-47R-6, 50-51	435.42	0.14	—		0.41	33	-0.01	0.11	1.17	82
1260B-37R-6, 62-63	445.04	0.61‡	—		0.34	39	-0.43	0.11	1.16	79
1260B-38R-6, 34-35	455.87	0.08	—		0.37	44	-0.77	0.05	0.79	85

Notes: \* = amount of sample digested with Na citrate-Na bicarbonate-dithionite (CBD) method is negligible. † = errors are expressed as two standard deviations around the mean for at least two independent measurements. ‡ = anomalously high values due to contaminated resin. AR = aqua regia. HF = hydrofluoric acid. — = not measured.